

Carrier lifetime reduction in 1.5 μm AlGaAsSb saturable absorbers with air and AlAsSb barriers

O. Ostinelli^{a)} and W. Bächtold

Department for Information Technology and Electrical Engineering, ETH Zurich, 8092 Zürich, Switzerland

H. Haiml, R. Grange, and U. Keller

Physics Department, Institute of Quantum Electronics, ETH Zurich, 8092 Zürich, Switzerland

E. Gini

FIRST Center for Micro- and Nanoscience, ETH Zurich, 8092 Zürich, Switzerland

G. Almuneau

LAAS-CNRS, 7 Av. Colonel Roche, 31077 Toulouse, France

(Received 11 January 2006; accepted 10 June 2006; published online 18 August 2006)

The optical properties of different AlGaAsSb semiconductor saturable absorber mirrors and InP/AlGaAsSb heterostructures have been investigated by pump-probe and low temperature photoluminescence measurements. The results show that the type-II electron-hole recombination process at the InP–AlGaAsSb interface is responsible for the slow carrier decay time in the absorber. Nevertheless, this slow transition can be avoided by growing an AlAsSb barrier layer between InP and the absorber layer promoting the fast electron-hole recombination at the surface states on the absorber/air interface. This allows reducing the carrier decay time from several nanoseconds down to 20 ps. © 2006 American Institute of Physics. [DOI: 10.1063/1.2240742]

High performance semiconductor saturable absorber mirrors (SESAMs) results from a balance of parameters such as the modulation depth, the saturation fluence, the inverse absorption, the nonsaturable absorption, and the carrier decay time.¹ By optimizing these parameters, we have recently demonstrated the first antimonide SESAMs, which self-started and mode locked an Er:Yb:glass laser at 61 MHz and 10 GHz repetition rates.² The SESAM structures consist of a 60-period InGaAsP/InP distributed Bragg reflector (DBR) and a 7-nm-thick AlGaAsSb absorber grown by metal-organic vapor-phase epitaxy (MOVPE).³ Due to the low intracavity power in multigigahertz repetition rate lasers, the SESAMs were designed with a low modulation depth in order to overcome the Q -switched mode locking threshold.⁴ Compared to other absorber materials, the AlGaAsSb material presents an Urbach absorption tail extending over about 70 meV below the band gap. This feature enables a fine tuning of the modulation depth below values of 0.5% by simply varying the composition of the quaternary alloy.⁵ A challenge, however, consists in the fabrication of AlGaAsSb absorbers with fast carrier decay times to achieve stable operation at high repetition rates. A growth temperature below 450 °C as in molecular beam epitaxy can lead to crystal defects, which make the SESAM faster.⁶ However, this method cannot be applied in MOVPE since a higher growth temperature (>550 °C) is required for the decomposition of the metal-organic sources. The creation of defects in the MOVPE grown absorbers is usually achieved by ion implantation.⁷ In our work, AlGaAsSb saturable absorbers with densities of droplet like surface defects up to 10^6 cm^{-2} and/or crosshatches and dislocations did not influence the carrier lifetime. Pump-probe measurements have revealed that the carrier decay time depends more on the band struc-

ture around the AlGaAsSb absorber rather than on the absorber crystal quality.

In the present letter, we report on the carrier recombination mechanisms in AlGaAsSb absorbers studied on different SESAM structures. The slow carrier decay time is caused by the type-II electron-hole recombination at the interface between InP and AlGaAsSb, which is unusual for SESAM structures.^{8,9} With different pump-probe measurements performed on a variety of structures, the principal mechanisms responsible for long carrier decay time were identified. We finally demonstrate that fast AlGaAsSb absorbers with a single exponential carrier decay time of 20 ps can be achieved.

The studied AlGaAsSb absorbers were deposited on InGaAsP/InP and AlGaAsSb/InP DBRs designed for the wavelength of 1.55 μm , with linear reflectivities of 99.9% and 99.6%, respectively.³ All the epitaxial layers were grown in a horizontal MOVPE reactor heated by halogen lamps at a pressure of 160 mbars and the temperatures ranging between 570 and 630 °C. The $\text{Al}_x\text{Ga}_{1-x}\text{As}_y\text{Sb}_{1-y}$ alloys were grown lattice matched to InP with $y=0.51$ and with high crystal quality. The band gap was tuned by changing the Al concentration between $x=0$ and $x=0.05$. Three different antimonide SESAMs have been grown with the aim of achieving fast saturable absorbers. The structure (a) consists of a 24-period InP/AlGaAsSb DBR, an InP spacer layer of 125 nm, and a 7-nm-thick $\text{Al}_{0.05}\text{Ga}_{0.95}\text{As}_{0.51}\text{Sb}_{0.49}$ absorber capped by 10 nm of InP. On this sample, measurements of the saturation fluence and the modulation depth gave $50 \mu\text{J}/\text{cm}^2$ and 0.4%, respectively. The structure (b) was obtained by etching the InP cap layer of the SESAM (a) with HCl diluted in phosphoric acid (H_3PO_4) (1:3). Finally, the SESAM structure (c) consists of a 60-period InGaAsP/InP DBR, a 75-nm-thick InP spacer, an AlAsSb barrier of 10 nm, and a $\text{GaAs}_{0.51}\text{Sb}_{0.49}$ absorber of 8 nm without InP cap. Figure 1 shows the conduction band (CB) and valence band (VB)

^{a)}Electronic mail: almuneau@laas.fr

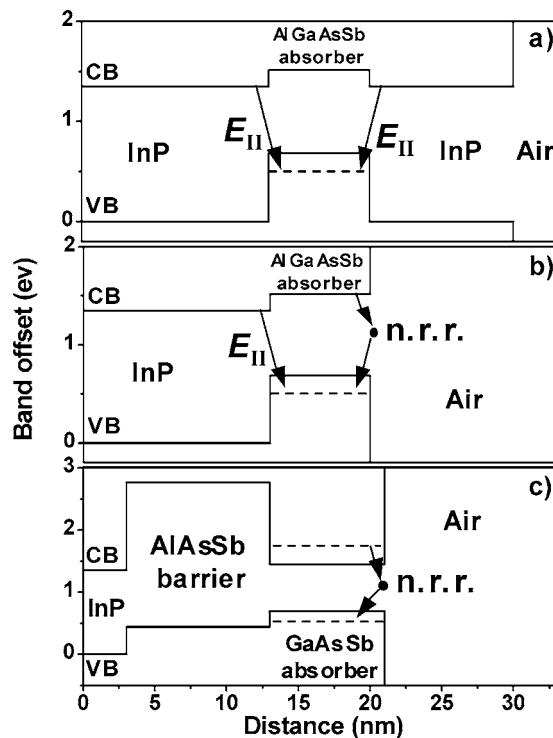


FIG. 1. Conduction and valence band near the absorber for three SESAMs: (a) 125 nm of InP, 7 nm of AlGaAsSb absorber, and 10 nm of InP; (b) SESAM (a) without InP cap; (c) 75 nm of InP, 10 nm of AlAsSb barrier, and 8 nm of GaAsSb absorber. I and II denote the type-I and type-II recombinations and “nrr” stands for the nonradiative recombination. The arrows show the allowed transitions.

diagrams versus the distance in growth direction for the top layers of the SESAMs [(a)–(c)]. The reference energy is represented by the InP VB. The CB and VB offsets are given by $\Delta E_{VB} = E_g(\text{InP}) - E_{II}$ and $\Delta E_{CB} = E_g(\text{AlGaAsSb}) - E_{II}$, respectively. $E_g(\text{InP})$ and $E_g(\text{AlGaAsSb})$ are the band gaps of InP and AlGaAsSb corresponding to the CB-to-VB transition (type-I) obtained from the 15 K photoluminescence (PL). E_{II} is the energy of the type-II PL emission caused by the recombination of the spatially separated electrons in the CB of InP and the holes in the VB of AlGaAsSb. Since the band offsets at 300 K varies by less than 0.020 eV when the temperature is increased from 15 to 300 K, the band offsets at 15 K were drawn in Fig. 1 together with the room temperature band gap energies. For the structures (a) and (b), ΔE_{CB} and ΔE_{VB} offsets between the $\text{Al}_{0.05}\text{Ga}_{0.95}\text{As}_{0.51}\text{Sb}_{0.4}$ absorber and InP are 0.159 and 0.685 eV, respectively. The absorber band gap energy is 0.838 eV. For the structure (c) the $\text{GaAs}_{0.51}\text{Sb}_{0.49}$ absorber shows a band gap of 0.78 eV, and the CB and VB offsets are 0.105 and 0.702 eV, respectively. The ΔE_{CB} and ΔE_{VB} between AlAsSb and InP are 1.349 and 0.441 eV.⁹ Pump-probe measurements have been performed on the SESAMs, with laser pulses of 3 ps duration at the wavelength of 1.535 μm and repetition rate of 61 MHz. The pump and probe fluences were set at 45 and 0.5 $\mu\text{J}/\text{cm}^2$, respectively. Figure 2(a) shows the normalized reflectivity change ΔR versus the time delay between the pump and the probe pulses for SESAM (a). The carrier decay time fitted by a single exponential decay is in the order of 1 ns. Similar decay time has been reported in a different staggered-band heterostructures on InP by Böhler *et al.*¹⁰ At $t=0$, the pump pulse generates electron-hole pairs. In the absence of reflections of the electron wave function at the

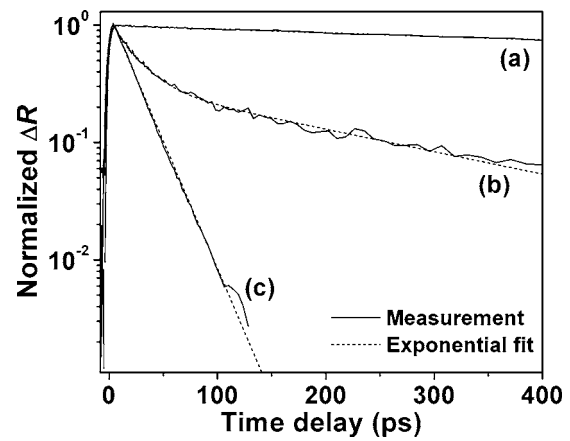


FIG. 2. Normalized reflectivity change ΔR vs time delay between pump and probe pulses for SESAMs [(a)–(c)] (solid lines). The measured reflectivity vs time has been fitted with an exponential decay (dashed lines).

interfaces, the delocalized electrons in AlGaAsSb can diffuse into the CB of InP. Since the holes are trapped in the VB quantum well, the separation between electrons and holes causes a bending of the CB and VB.¹¹ The resulting U-shaped AlGaAsSb CB can confine electrons, which increases the probability for a direct (type-I) transition in the absorber. For the thin saturable absorber of 7 nm, however, the number of electrons undergoing such direct transition is very low and the type-II recombination across the interface dominates. As the absorber width increases the probability for the type-I transition increases. This has been demonstrated by the 15 K PL spectra of two $\text{Al}_{0.05}\text{Ga}_{0.95}\text{As}_{0.51}\text{Sb}_{0.4}$ embedded between InP with layer thicknesses of 7 and 100 nm (see Fig. 3). For the AlGaAsSb bulk both type-I and type-II transitions are visible. On the other hand, for the quantum well like saturable absorber layer the spatially indirect transition clearly dominates. Similar results have been reported by other authors.¹² The slow carrier decay time in SESAM (a) is thus attributed to the type-II recombination across the InP–AlGaAsSb interfaces. This spatially indirect recombination is shown in Fig. 1. For SESAMs with absorbers showing three-dimensional defects, the carrier decay time was in the same order of magnitude.⁵

The pump-probe measurement performed on SESAM (b) shows a fast carrier decay time, followed by a slower one

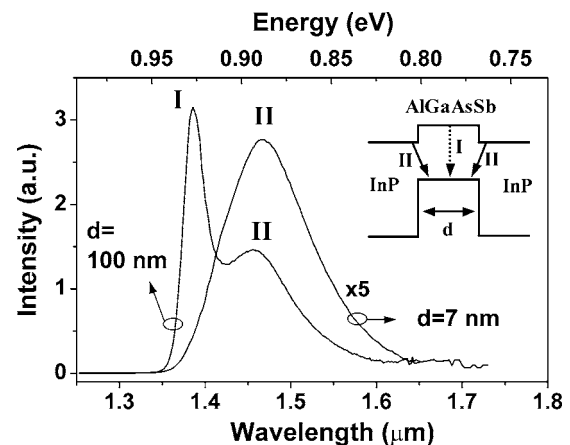


FIG. 3. Photoluminescence spectrum at 15 K of $\text{Al}_{0.05}\text{Ga}_{0.95}\text{As}_{0.51}\text{Sb}_{0.49}$ with thicknesses of (a) 100 nm and (b) of 7 nm. AlGaAsSb is embedded between InP (inset). The type-I and type-II emissions are denoted as I and II.

[Fig. 2(b)]. At the InP/AlGaAsSb interface (interface 1) the electrons undergo a type-II transition by recombining with the holes in AlGaAsSb. A part of the photogenerated carriers, however, diffuses towards the AlGaAsSb/Air interface (interface 2) and recombine at the surface states. This also occurs when a thin (2 nm) InP layer caps the SESAM, as reported by Garnache *et al.*¹³ Assuming that at each interface a group of spatially separated electrons is formed, ΔR is described by $A_1 \exp(-t/\tau_1) + A_2 \exp(-t/\tau_2)$. τ_1 is the carrier decay time at interface 1 and τ_2 that at interface 2. A_1 and A_2 represent the probability at $t=0$ for the electrons to be around interfaces 1 and 2, respectively. This implies that $A_1 + A_2 = 1$. By fitting curve (b) yields $A_1 = 0.31$ and $A_2 = 0.69$ and $\tau_1 = 227$ ps and $\tau_2 = 22$ ps. About 30% of the carriers are involved in a slow type-II transition at interface 1, and 70% rapidly recombine at the surface states of interface 2. The faster type-II transition in sample (b) (227 ps) compared to sample (a) (1 ns) might be due to the diffusion of surface states created after the wet etch. A second possibility for the different decay times would be the different band bendings induced by the air interface and its surface states, which would result in different overlaps of electron and holes wave functions. This effect has been reproduced for different growth runs with nominally the same structure.

To further decrease the carrier decay time, a 10-nm-thick AlAsSb layer was grown between the InP spacer layer and the GaAsSb absorber layer [structure (c)] to avoid the slow type-II transition observed in SESAM (b). The AlAsSb layer forms a barrier for the electrons in the CB of GaAsSb, which impedes their diffusion into the CB of InP. In structure (c) the electrons occupy the first excited subband in the GaAsSb absorber well. The solution of the Schrödinger equation for an 8-nm-thick GaAsSb saturable absorber with an AlAsSb/GaAsSb CB offset of 1.349 eV and an air energy barrier of infinite height gives an electron energy level lying about 90 meV above the Γ band minimum of GaAsSb. The Coulomb interaction between electrons and holes has been neglected. The fitted carrier decay time in SESAM (c) is of 20 ps only [see Fig. 2(c)]. This fast decay time is attributed to the recombination process at the surface states on the

GaAsSb/Air interface and is in very good agreement with $\tau_2 = 22$ ps of SESAM (b).

In summary, the relaxation times in AlGaAsSb saturable absorber were investigated by pump-probe measurements. The slow carrier decay time observed for SESAMs composed of AlGaAsSb absorbers embedded between InP layers is due to the recombination of electrons and holes localized in InP and AlGaAsSb, respectively. Selectively etching of the InP cap leads to a significant reduction of the carrier decay time. A fast carrier decay time of 22 ps has been attributed to the recombination at surface states on the AlGaAsSb/Air interface. Beside the fast decay time, however, a slower decay time of 227 ps was caused by the type-II transition across the InP/AlGaAsSb interface. To further reduce the relaxation time, an AlAsSb has been grown between the InP spacer and the absorber layer. As a result, a fast SESAM with carrier decay times as low as 20 ps has been achieved.

The authors would like to acknowledge M. Ebnöther for the contribution on the MOVPE growth.

¹U. Keller, *Nature (London)* **424**, 831 (2003).

²R. Grange, O. Ostinelli, M. Haiml, L. Krainer, G. J. Spühler, S. Schön, M. Ebnöther, E. Gini, and U. Keller, *Electron. Lett.* **40**, 1414 (2004).

³O. Ostinelli, H. Haiml, R. Grange, G. Almuneau, M. Ebnöther, E. Gini, E. Müller, U. Keller, and W. Bächtold, *J. Cryst. Growth* **286**, 247 (2005).

⁴C. Hönninger, R. Paschotta, F. Morier-Genoud, M. Moser, and U. Keller, *J. Opt. Soc. Am. B* **16**, 46 (1999).

⁵R. Grange, S. C. Zeller, S. Schön, M. Haiml, O. Ostinelli, M. Ebnöther, E. Gini, and U. Keller, *IEEE Photonics Technol. Lett.* **18**, 805 (2006).

⁶M. Haiml, U. Siegner, F. Morier-Genoud, U. Keller, M. Luysberg, R. C. Lutz, P. Specht, and E. R. Weber, *Appl. Phys. Lett.* **74**, 3134 (1999).

⁷H. H. Tan, C. Jagadish, M. J. Lederer, B. Luther-Davies, J. Zou, D. J. H. Cockayne, M. Haiml, U. Siegner, and U. Keller, *Appl. Phys. Lett.* **75**, 1437 (1999).

⁸M. Peter, N. Herres, F. Fuchs, K. Winkler, K.-H. Bachem, and J. Wagner, *Appl. Phys. Lett.* **74**, 410 (1999).

⁹O. Ostinelli, G. Almuneau, and W. Bächtold, *Semicond. Sci. Technol.* **21**, 681 (2006).

¹⁰J. Böhrer, A. Krost, and D. Bimberg, *Appl. Phys. Lett.* **64**, 1992 (1994).

¹¹T. Baier, U. Mantz, K. Thonke, F. Schäffler, R. Sauer, and H.-J. Herzog, *Phys. Rev. B* **50**, 15191 (1994).

¹²T. Mozume, N. Georgiev, H. Yoshida, A. Neogi, and T. Nishimura, *J. Vac. Sci. Technol. B* **18**, 1586 (2000).

¹³A. Garnache, S. Hoogland, I. Sagnes, G. Saint-Girons, J. S. Roberts, and A. C. Tropper, *Appl. Phys. Lett.* **80**, 3892 (2002).